DOI: 10.1021/ma9011126

Macromolecules
ARTICLE

Poly(Z-lysine)-Based Organogels: Effect of Interfacial Frustration on Gel Strength

Sandeep S. Naik[†,‡] **and Daniel A. Savin***[,†]

[†]*School of Polymers and High Performance Materials, University of Southern Mississippi, Hattiesburg, Mississippi 39406, and* [‡]*Department of Chemistry, University of Vermont, Burlington, Vermont 05405*

Received May 21, 2009; Revised Manuscript Received August 12, 2009

ABSTRACT: A series of poly(Z-lysine)-based block copolymers were synthesized with poly(propylene oxide), poly(ethylene oxide-*stat*-propylene oxide), and polyhedral oligomeric silsesquioxane. These copolymers form thermoreversible gels in tetrahydrofuran with critical gel concentrations as low as 0.5 wt %. Infrared spectroscopy indicates that the peptide block adopts an antiparallel β-sheet conformation whereby the assembly is facilitated by intermolecular H-bonding. The modulus of the gels was determined as a function of poly(Z-lysine) molecular weight and solution concentration (1−4 wt %). It was found that increasing the poly(Z-lysine) molecular weight or concentration increases gel strength and the range of linear viscoelastic response with stress. Remarkably, gel strengths as high as 220 and 348 Pa in THF and chloroform, respectively, were observed. In addition, the gel strength is highly dependent on the solvent interactions with the non-peptide block of the copolymer. We propose a model where interfacial frustration destabilizes β-sheet assembly of peptide block, leading to weaker gel.

Introduction

Gels are soft materials containing a three-dimensional network of molecules or aggregates that trap either an aqueous phase (hydrogel) or an organic phase (organogel). Although gels are primarily composed of liquid, they exhibit solidlike properties in terms of their mechanical response. In general, the network formation occurs through cross-linking between chains or physically through entanglements of self-assembled supramolecular structures. Early work by Weiss focused on fibril networks formed from the self-assembly of small-molecule gelators to form physical gels in organic solvents.[1,2] Similarly, recent work by Pochan and others has demonstrated physical hydrogel formation from the assembly of small oligopeptide-based materials into molecular fibril networks.[3,4]

Peptides are fascinating materials, as they exhibit various secondary structures (i.e., α-helix and β-sheet) under different solution conditions. Recent work by the Savin group has focused on exploiting secondary structure transitions to produce pH and temperature-responsive micelles and vesicles.[5,6] Peptide-based hydrogels form as a result of ionic interactions, hydrophobic association, or coiled-coil interactions.[7−9] One classic example comes from the "leucine zipper" mechanism of assembly.[10] More recently, Deming and Pochan have focused on hydrogels based on copolypeptides or β-hairpin peptides, respectively, which find application in soft tissue engineering.[3,4,11,12] Deming and Manners propose a nanoribbon assembly motif whereby the peptide helices assemble in a direction normal to the fibril direction.[13,14] In many of these hydrogel systems, the peptide component is hydrophobic (i.e., leucine or valine) and retains an α-helical structure, and the driving force for assembly comes from the hydrophobic effect.

Organic liquid-based gels have opened up various new applications which are not possible with hydrogels. Organogels derived from low molecular weight organic compounds have been around for some time and have potential applications as nanostructure directing agents and functional materials.[15−23] Similar to hydrogels, peptide-based organogels form typically through noncovalent interactions such as hydrogen bonding, van der Waals interactions, $\pi-\pi$ stacking, and solvophobic interactions.[24−28] Escuder et al. give an example of tetrapeptide-based low-molecular-weight gelators that self-assemble to yield organogels.[29]

The functionality of peptide-based organogels can be enhanced by attaching the assembling peptide block to a synthetic polymer block or dendrimer, which then results in formation of various three-dimensional supramolecular arrangements, as shown by Stupp and others.[11,13,21,26,30] In this assembly motif, the nonpeptide block serves to facilitate dispersion of the assembled fibrils in the organic solvent. Rod−coil block polymers based on poly(γ-benzyl glutamate) (PBLG) have been used extensively for this purpose.[14,31−34] Note that PBLG consists of a hydrophilic peptide containing a side-chain-protected carboxylic acid group. PBLG is a model rodlike polypeptide which can assume an α-helical or a β-sheet secondary structure depending on solution conditions and molecular weight. Komoto and his group synthesized a thermoplastic hydrogel based on hexablock copolymer composed of PBLG and poly(ethylene oxide) (PEO).[35] Yang et al. report hydrogel formation in diblock copolymers of PBLG and PEO. They showed that in these hydrogels the secondary structure of the PBLG block has a significant effect on the swelling ability of the gel.[24] Finally, Manners and coworkers have reported dendron−PBLG thermoreversible gels in toluene.[36] It has been established that the assembly motif in peptide-based organogels comes from assembly into a fibril network, and it should be noted that the peptide does not necessarily retain its secondary structure. For example, Boerner and coworkers report a sequence-defined polypeptide block copolymer with poly(*n*-butyl acrylate) which adopts an antiparallel β-sheet motif, forming a tapelike morphology in organic solvents.[37] In all of these cases the assembly of the peptide segments induces microstructure formation in the synthetic polymer attached to it.

*Corresponding author. E-mail: daniel.savin@usm.edu.

 Published on Web 08/25/2009

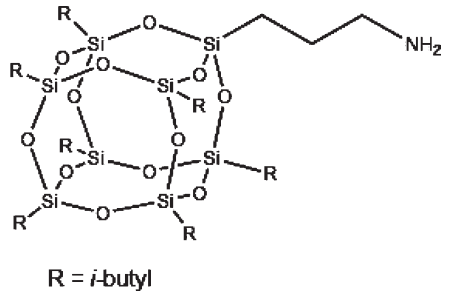

Figure 1. Structure of POSS-NH_2.

Herein we report the synthesis and viscoelastic properties of organogels based on poly(Z-lysine) P(Lys(Z)). In these materials, the side-chain amine groups of the lysine units are protected, resulting in a hydrophobic peptide similar to PBLG discussed above. P(Lys(Z)) can exhibit either an α-helical or a β-sheet conformation in organic solvent. We have synthesized block copolymers of P(Lys(Z)) with poly(propylene oxide) (PPO), statistical copolymers of ethylene oxide and propylene oxide (Jeffamines), and polyhedral oligomeric silsesquioxane (POSS), a small hydrophobic cage molecule. Our goal is to determine how the structure and solvent interactions with the non-peptide block affect gel strength and the range in the linear viscoelastic response. In contrast to PBLG organogels, P(Lys(Z)) organogels remain largely unexplored. Work has been done by Smith and co-workers on lysine-based dendritic organogelators.[38,39] While these previous studies have focused on the structure of the organogels, we intend to focus on the rheological properties.

Experimental Section

Materials. Dimethylformamide (DMF, Alfa Aesar) and tetrahydrofuran (THF, Fisher) were distilled from molecular sieves and sodium/benzophenone, respectively, and degassed before use. Triphosgene (Acros) and tosyl chloride (Acros) were used without further purification. H-Lys(Z)-OH was purchased from EMD Novabiochem, and its *N*-carboxyanhydride (NCA) was prepared according to previously reported methods.[5,6] Poly(propylene oxide), monobutyl ether (PPO−OH, Aldrich, M_n = 2500 g/mol, DP_n=44), was used as received. Jeffamines M-2005 ($PEOPO_{6-29}$) and M-2070 ($PEOPO_{10-31}$) were provided by Huntsman Chemicals and used as received. Jeffamines are monoamine-functionalized statistical copolymers of ethylene oxide (EO) and propylene oxide (PO). The subscripts denoted above give the DP_n of EO and PO, respectively, in the copolymer. Aminopropylisobutyl-polyhedral oligomeric silsesquioxane (POSS-NH_2) (Figure 1) was generously donated by Hybrid Plastics (Hattiesburg, MS) and was used as received. Other solvents such as diethyl ether, pyridine, and methanol (Fisher) were used as received.

Synthesis. *General Strategy*. The general scheme for producing copolymers containing P(Lys(Z)) blocks is given in Scheme 1. Primary amine-functionalized macroinitiator is used in the ring-opening polymerization of the *N*-carboxyanhydride of lysine(Z) (Lys(Z)-NCA). In these studies, the POSS and Jeffamine samples contain the amine functionality and can be used directly. Hydroxy-functionalized PPO−OH was converted to an amine as discussed below.

Synthesis of Amine-Terminated Poly(propylene oxide) (*Scheme 2*). PPO−OH (10 g, 4 mmol) was dissolved in 50 mL of pyridine, and tosyl chloride (7 g, 40 mmol) was added to the solution. The reaction mixture was stirred for 24 h at room temperature and then poured into 50 mL of a 6 M HCl solution. The product was extracted with methylene chloride, which was removed under vacuum. The polymer was then precipitated in cold diethyl ether and dried for 24 h under vacuum. The monotosylated polymer was then dissolved in DMF, and

Scheme 1. Ring-Opening Polymerization of Lys(Z)-NCA Using an Amine-Functionalized Macroinitiator

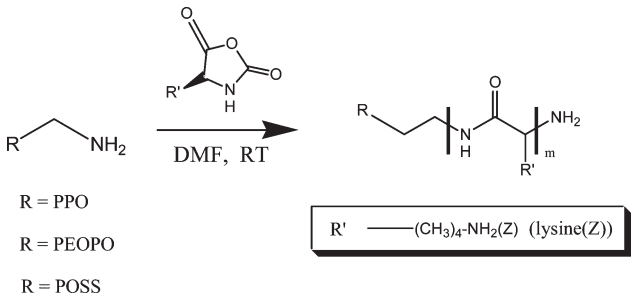

sodium azide (10 equiv) was added to the solution. The reaction mixture was stirred at 40 °C for 24 h. **Care must be taken such that the temperature not exceed 60 °C, as the azide becomes extremely shock sensitive.** The reaction mixture was filtered to remove excess undissolved sodium azide and then poured into a solution of cold 6 M HCl. The product was extracted using methylene chloride, and the organic layer was again washed with 150 mL of cold water. The product obtained is then dried under vacuum overnight. The yield of this reaction is about 90%. The terminal azide group is then reduced to an amine via hydrogenation in presence of 10% Pd/C catalyst.

Synthesis of Lys(Z) N-Carboxyanhydride (*Lys(Z)-NCA*). The synthesis of Lys(Z)-NCA was performed using a method described previously.[5,6] Briefly, H-Lys(Z)-OH (10 g, 35.7 mmol) was introduced in to a flame-dried flask and dissolved into THF to a final concentration ca. 0.1 g/mL. The slurry was stirred at 55−60 °C for 20 min under nitrogen. Triphosgene (5.12 g, 17.25 mmol) dissolved in 10 mL of THF was introduced into the H-Lys(Z)-OH slurry under a steady flow of nitrogen, and a drying tube was attached to the reactor. After about 1 h, the reaction became clear. The reaction mixture was concentrated via rotovap and precipitated into hexanes overnight. The precipitate was then redissolved in THF, and 1 g of decolorizing charcoal was added and stirred overnight to eliminate residual hydrochloric acid. The reaction mixture was then passed through a Celite column to remove charcoal, concentrated, and reprecipitated into hexanes overnight at low temperature. The white powder formed is then dried under vacuum overnight to obtain Lys(Z)-NCA. Typical yields were between 85 and 92%.

Synthesis of Block Copolymers. Block copolymerization was carried out by the ring-opening polymerization of Lys(Z)-NCA using the corresponding amine-functionalized macroinitiator in DMF for 5 days at room temperature. The polymer was then precipitated in ether, redissolved in chloroform, and reprecipitated in cold ether to remove any unreacted macroinitiator.

Preparation of Organogels. Peptide-based organogels are usually prepared by warming the gelators in organic liquid until the solid dissolves, followed by cooling the solution below the gel transition temperature.[15,20] In contrast to this protocol, the systems presented here only require efficient mixing at room temperature to obtain gels with a gel−sol transition above the boiling point of THF.

Organogels were prepared by directly mixing the block copolymer in organic solvent, followed by rigorous sonication. The homogeneous gels were allowed to stand for an hour, and the gelation was confirmed qualitatively by the inverted test tube method. We define the critical gelation concentration (CGC) as the lowest concentration of polymer that would form organogels under these conditions. Organogels were prepared with concentrations between 0.5 and 4 wt % in THF or chloroform.

Molecular Characterization. ^{1}H NMR spectra were recorded on Varian Mercury 300 (300 MHz) spectrometer. NMR solvents with 1% v/v TMS were used for internal standardization. Molecular weight distributions of the polymers synthesized were

Scheme 2. Preparation of Amine-Terminated PPO from PPO−OH

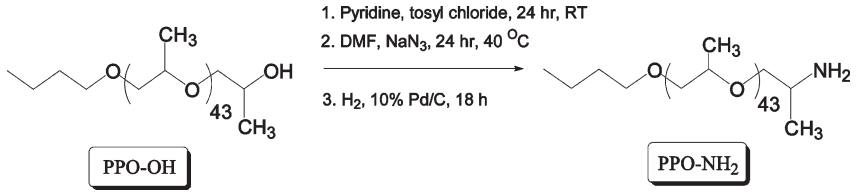

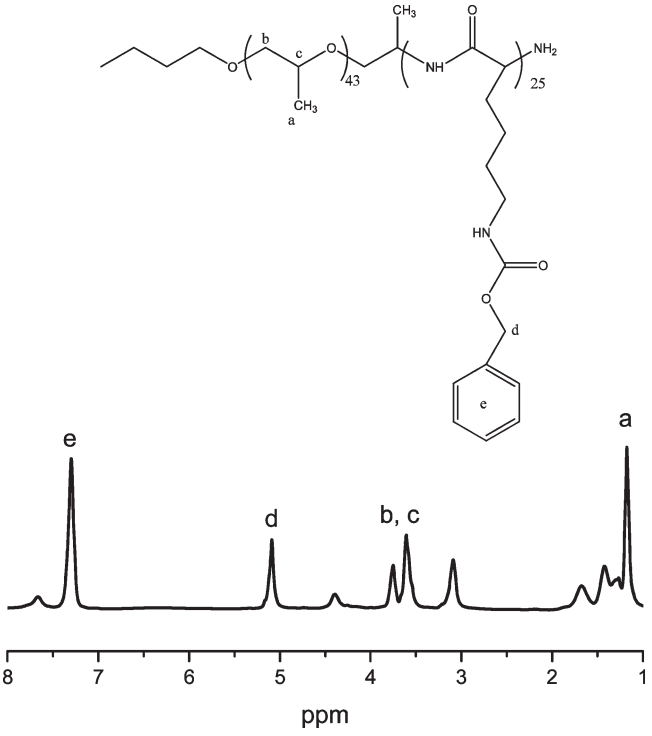

Figure 2. ^{1}H NMR spectrum of a PPO-P(Lys(Z)) block copolymer with a target block ratio of 44:25. To determine actual composition, the integration at $\delta = 1.1$ ppm is compared with the integration at $\delta = 5.05$ ppm.

determined using size exclusion chromatography (SEC) with a Viscotek TDA 302, fitted with two low molecular weight columns connected in series. DMF with 0.02 M ammonium acetate was used as eluent at a flow rate of 1 mL/min. The SEC was operated at 35 °C. FTIR spectra were recorded on Bruker Equinox 55 instrument. The samples were placed between two KBr plates or pressed into disks and held in the sample chamber under a steady flow of nitrogen. Four sets of 32 scans were recorded with spectral resolution of 4 cm^{-1} and averaged, subtracting KBr and THF spectra from the sample spectra. The analysis was performed using OPUS 6.5 software provided by Bruker.

Scanning Electron Microscopy (SEM). SEM images of xerogels were taken using an FEI Quanta 200 FEG instrument. Gel samples were placed on an aluminum stub which was suspended in liquid nitrogen to freeze the organogel samples. The stubs were immediately transferred to a freeze-dryer to slowly remove solvent from the sample without disturbing the gel structure. The samples were gold sputtered for 2 min to increase the contrast. Typical magnifications were 4000× at 20.0 kV.

Rheology. The mechanical properties of the organogels were studied using an AR G2 controlled-stress rheometer (TA Instruments) with a 40 mm crosshatched parallel plate geometry. Testing consisted of three sequential measurements. First, a stress sweep was performed from 0.1 to 100 Pa at a frequency of 1 Hz. Then, the recovery of the gel after a rigorous (6 rad/s, 2 min) preshear was measured as a function of time under a stress of 0.1 Pa. Finally, a frequency sweep (0.1 or 0.1−10 Hz) was performed on the recovered gel under a stress of 0.1 Pa. The temperature of the peltier plate was maintained at 2 °C to prevent rapid evaporation of THF. We quantify the gel strength via the shear storage modulus (G').

Table 1. Block Ratios for Organogel-Forming Polypeptide Block Copolymers

sample	target DP_n for P(Lys(Z))	actual DP_n (NMR)
PPO_{44}−$P(Lys(Z))_{27}$	25	27
PPO_{44}−$P(Lys(Z))_{43}$	50	43
PPO_{44}−$P(Lys(Z))_{112}$	100	112
POSS-$P(Lys(Z))_{20}$	20	20
POSS-$P(Lys(Z))_{38}$	40	38
$PEOPO_{6-29}$-$P(Lys(Z))_{57}$	50	57
$PEOPO_{6-29}$-$P(Lys(Z))_{110}$	100	110
$PEOPO_{10-31}$-$P(Lys(Z))_{30}$	50	30

Results and Discussion

Synthesis. The block ratios of the polymers were determined by ^{1}H NMR spectroscopy in $CDCl_3$ + 15% (w/w) trifluoroacetic acid (TFA). The addition of TFA serves to facilitate dissolution into $CDCl_3$. Figure 2 shows a representative NMR spectrum of PPO-P(Lys(Z)). To determine number-averaged block ratios, the integration of the peak at $\delta = 1.1$ ppm (a, due to methylene protons from the PPO block) is compared with the peak at $\delta = 5$ ppm (d, due to benzyl protons of the protecting group.) Since the proton resonances for POSS are all around $\delta = 0$ ppm, and the exact composition of PPO in the Jeffamines is not known, block ratios were determined by comparing the methylene protons α to the amine termini with the benzyl protons of the protecting group as above. Table 1 shows the target and actual block ratios of the polymers studied. The polydispersities for the polymers were between 1.3 and 1.5, typical for NCA ring-opening polymerizations.

Structure of Organogels and the Driving Force for Organogelation. Previous literature on peptide-based organogels has established that gelation occurs via formation of extended structures (i.e., nanoribbons) from the assembly of the solventphobic peptide helices.[13,33,36] This begins with disruption of the solid-state structure, followed by reorganization of the geling materials. With typical small-molecule organogelators this is achieved by heating the material and then cooling below the critical gel temperature. In the case of organogels in THF, the critical gel temperature (ca. 77 °C) is above the boiling point of the solvent; thus, sonication is used for the initial disruption. Restructuring occurs via a hierarchical assembly process as suggested by Hentschel and Boerner.[37] We propose that for P(Lys(Z))-based block copolymers peptide self-assembly is driven by hydrogen bond formation to form β-sheets which further stack to form ribbons which can further aggregate to form fibers. This hierarchical self-assembly can form larger aggregates which are enriched by solvent molecules leading to gel formation, and the resultant structures span dimensions up to micrometers. Solventphilic side chains play important role in filling gaps on the surface of β-sheets, especially aromatic group; thus, the protecting group on the lysine side chains

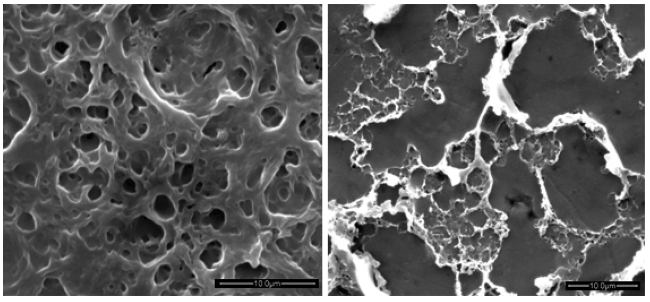

Figure 3. SEM images for xerogels of P(Lys(Z))-based block copolymers. Left: 0.5 wt % POSS-P(Lys(Z))$_{20}$ from THF. Right: 1 wt % PPO$_{44}$-P(Lys(Z))$_{112}$ from THF. The lower concentration of POSS-P(Lys(Z)) clearly exhibits a network structure that is more dense compared with PPO-P(Lys(Z)). Scale bar is 10 μm in both images.

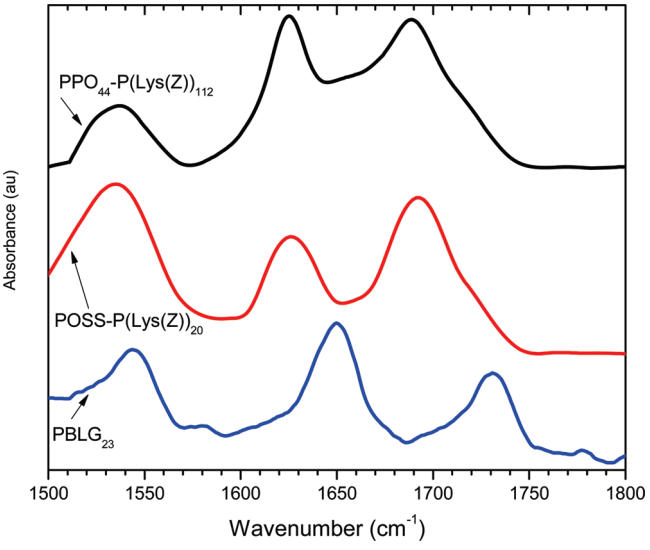

Figure 4. FTIR spectra of P(Lys(Z))-based organogels. Top: 1 wt % PPO$_{44}$-P(Lys(Z))$_{112}$ in THF. Middle: 1 wt % POSS-P(Lys(Z))$_{20}$ in THF. Bottom: PBLG$_{23}$ for comparison. For the P(Lys(Z)) organogels, the signature in the amide region suggests an antiparallel β-sheet conformation of the P(Lys(Z)) blocks.

may facilitate gelation. In addition, terminal amine groups from the peptide may facilitate H-bonding for shorter peptide chains. SEM images for xerogels of POSS-P(Lys(Z)) and PPO-P(Lys(Z)) are shown in Figure 3. It is clear from these images that the network for POSS-P(Lys(Z)) is well-defined compared with PPO-P(Lys(Z)).

FTIR spectroscopy provides a fair insight into the orientation of the peptides, which can be helpful to support the cause for the gelation for these systems. Figure 4 shows the FTIR spectra for three systems: PPO$_{44}$-P(Lys(Z))$_{112}$ (1 wt % in THF), POSS-P(Lys(Z))$_{20}$ (1 wt % in THF), and PBLG, which is used as a helix standard in the solid state.[34] In general, the characteristic bands for hydrogen-bonded amide groups appear near 3286 cm^{-1} (amide A, υN−H not shown), 1633 cm^{-1} (amide I, υC═O), and 1543 cm^{-1} (amide II, δN−H). The amide II band is less dependent on secondary structure and for all three samples occurs at the same frequency. The amide I carbonyl stretching vibration can be used to (1) determine the presence of α-helix vs β-sheet secondary structure and (2) differentiate between antiparallel and parallel β-sheet structures.[29,40] From Figure 4, the amide I band that appears at 1625 cm^{-1} suggests that the P(Lys(Z)) adopts a β-sheet conformation in the organogel. This is in contrast to the PBLG α-helix where the carbonyl stretch occurs as a strong band at 1650 cm^{-1}. The absence of a band at 1645 cm^{-1} for

Table 2. Critical Gelation Concentrations and Gel Strengths for P(Lys(Z)) Organogels in THF

sample	CGC (wt %)	G' (Pa) for 4 wt % or 2 wt % (*) solutions
PPO$_{44}$-P(Lys(Z))$_{27}$	4	2.5
PPO$_{44}$-P(Lys(Z))$_{43}$	3	43
PPO$_{44}$-P(Lys(Z))$_{112}$	1	220
POSS-P(Lys(Z))$_{20}$	0.5	70*
POSS-P(Lys(Z))$_{38}$	0.5	170*
PEOPO$_{6-29}$-P(Lys(Z))$_{57}$	3	9
PEOPO$_{6-29}$-P(Lys(Z))$_{110}$	3	33
PEOPO$_{10-31}$-P(Lys(Z))$_{30}$	N/A	N/A

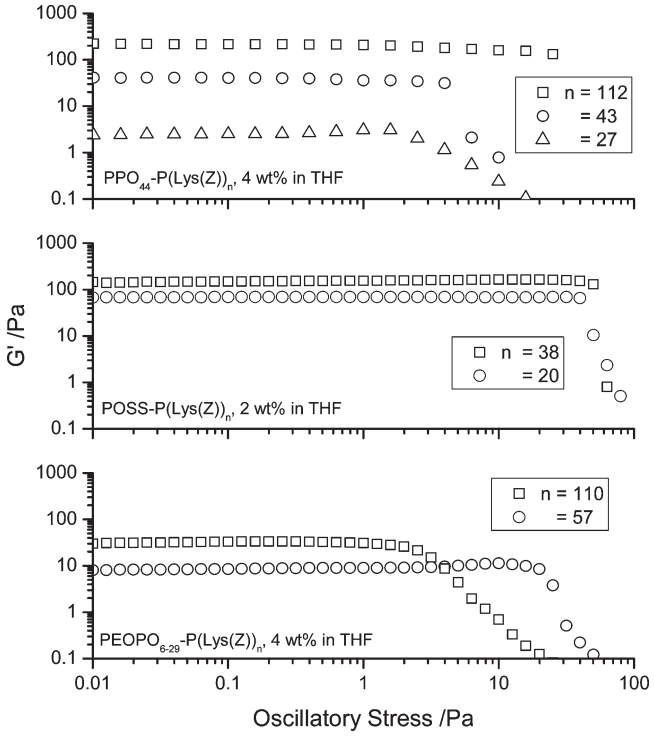

Figure 5. Stress sweeps for organogelating systems with varying molecular weight: (top) 4 wt % PPO$_{44}$-P(Lys(Z))$_n$ in THF; (middle) 2 wt % POSS-P(Lys(Z))$_n$ in THF; (bottom) 4 wt % PEOPO$_{6-29}$-P(Lys(Z))$_n$ in THF. Data were taken at 1 Hz and 2 °C.

P(Lys(Z)) suggests that the peptides do not adopt a parallel β-sheet. An antiparallel sheet would exhibit a weak band at 1690 cm^{-1} but is overshadowed by the carbonyl stretching from the Z protecting group in this region.[41] These results suggest that the PPO$_{44}$-P(Lys(Z))$_{112}$ organogels in THF adopt a predominantly antiparallel β-sheet structure where the assembly is facilitated by intermolecular hydrogen bonding. It is interesting to note that the PPO-P(Lys(Z)) spectrum exhibits a slight helical character (subtle shoulders in the peaks), but the dominant secondary structure is a β-sheet. The spectrum for POSS-P(Lys(Z)) exhibits almost no helical character. Previous literature suggests that there may be other stabilization mechanisms present. For example, β-sheet structures can be further stabilized due to the $\pi-\pi$ interactions between the protecting groups of the peptide.[42] Previous studies have focused on this effect in PBLG organogels; however, there are relatively few studies of P(Lys(Z)) to compare with here.

The β-sheet conformation is energetically favorable for P(Lys(Z)) in the dry state (prior to mixing with organic solvent) because it has strong intermolecular hydrogen bonds and requires a low degree of solvation.[43] When THF or another solvent is added, potentially the peptide block

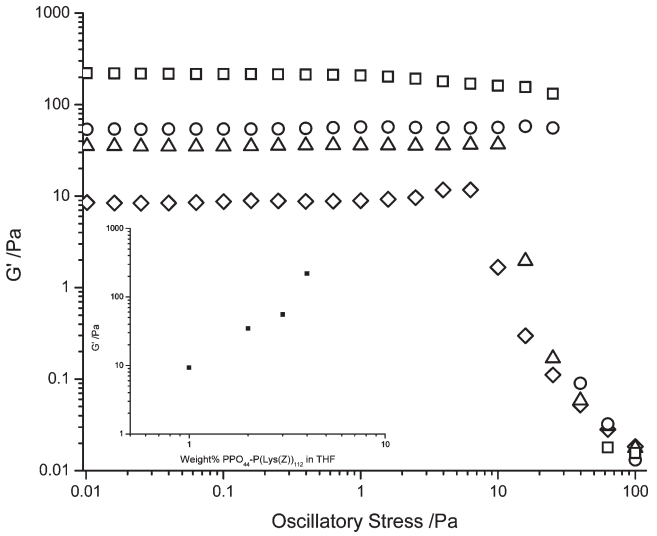

Figure 6. Stress sweeps for PPO_{44}-$P(Lys(Z))_{112}$ organogelating systems in THF with varying concentration: (□) 4, (○) 3, (Δ) 2, and (◇) 1 wt %. Data were taken at 1 Hz and 2 °C. Inset shows the dependence of gel modulus on concentration.

would have the freedom adopt an α-helix or random coil configuration, but the FTIR here shows that it still arranges itself into an antiparallel β-sheet conformation, leading to gelation. Note that assembly into a parallel β-sheet formation would cause distortion in the intermolecular hydrogen bonds. Given that the intermolecular β-sheet formation between P(Lys(Z)) blocks facilitates gelation in these systems, it is possible that the nature of the nonpeptide (corona block) may have a role on gel strength. For example, factors that lead to steric crowding at the interface of the assembly may disrupt the ability for β-sheet blocks to assemble intermolecularly.[44]

Mechanical Properties of Organogels. We have studied the organogel strength of P(Lys(Z)) block copolymers with PPO, PEOPO, and POSS in THF as a function of concentration and molecular weight of the peptide block. In general, we find that the critical gelation concentration (determined qualitatively with the inverted test tube method) decreases with increasing molecular weight of P(Lys(Z)) (Table 2). In addition, the time required for the gel to set after sonication decreases with increasing P(Lys(Z)) content. All gels undergo a gel−sol transition around 77 °C (above the boiling point of THF) but revert back to its original state after cooling down to room temperature without any significant weight loss. This suggests that there may be a thermal denaturation process that leads to gel breakdown.

Effect of P(Lys(Z)) Molecular Weight and Concentration on Organogel Strength. Figure 5 shows stress sweeps for P(Lys(Z)) block copolymer organogels for different molecular weights. In general, for all block copolymers studied the organogel strength increases with increasing P(Lys(Z)) block length when keeping the non-peptide block length (i.e., PPO, PEOPO, or POSS) constant. For 4 wt % solutions of PPO_{44}-$P(Lys(Z))_n$ block copolymers in THF (top of Figure 5), the gel strength increases from 2.5 to 43 Pa to 220 Pa for $n = 27$, 43, and 112, respectively. Generally, POSS-$P(Lys(Z))_n$ organogels (middle) exhibited a much greater strength compared with PPO-P(Lys(Z)) above. For 2 wt % solutions in THF, the gel strength increased from 70 to 170 Pa for $n = 20-38$. In fact, it was difficult to synthesize POSS-P(Lys(Z)) copolymers with higher P(Lys(Z)) content because the polymerization mixture gels prior to full conversion. For example, in chloroform (one of the polymerization solvents used),

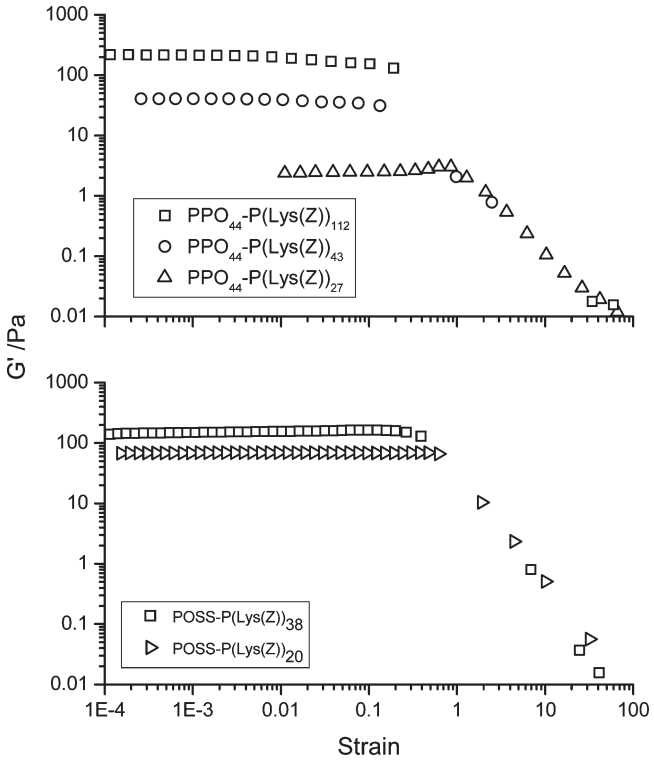

Figure 7. Strain sweeps for PPO-P(Lys(Z)) in THF (top) and POSS-P(Lys(Z)) in THF (bottom) organogels. The data presented are the same as those presented in stress sweeps (Figure 4), replotted with strain on the abscissa. In the region with strain higher than the critical strain, the data appear to superpose for both organogelating systems. Data were taken at 1 Hz and 2 °C.

$POSS\text{-}P(Lys(Z))_{38}$ copolymers have gel strengths as high as 348 Pa for 2 wt % solutions. Potentially, the solvent interaction between POSS and chloroform is more favorable compared with THF, which helps to stabilize nanoribbons in solution. Finally, $PEOPO_{6-29}$-$P(Lys(Z))_n$ copolymers (bottom) exhibited weak gels in THF, with strengths of 9 and 33 Pa for $n = 57$ and 110, relatively large P(Lys(Z)) block lengths compared with the other two systems. The other Jeffamine-based copolymer, $PEOPO_{10-31}$-$P(Lys(Z))_{30}$, did not form gels over the concentration range studied (up to 4 wt %.)

Figure 6 shows stress sweeps for PPO_{44}-$P(Lys(Z))_{112}$ organogels in THF as a function of concentration. The inset of Figure 6 shows the increase in gel strength as a function of concentration. As the concentration of the solutions is raised from 1 to 4 wt %, the gel strength increases from 9.3 to 220 Pa with a power law exponent of 2.1, consistent with gels of semiflexible polymers (inset).

We discuss these rheological results in terms of the changes in gel strength as a function of molecular weight and concentration as well as the range in the linear response with stress (plateau region prior to thinning.) The changes in gel strength as a function of concentration and molecular weight are not unexpected. Given that the assembly is dictated by intermolecular hydrogen bonding into fibrils as described above, as the molecular weight of the P(Lys(Z)) block is increased, the modulus of the gel may be expected to increase as well due to the stronger interactions between assembling P(Lys(Z)) chains. As shown in Figure 4, the modulus increased with molecular weight of the P(Lys(Z)) block for all systems studied. In terms of concentration, as the block copolymer content increases, we expect the modulus to increase, through either formation of longer fibrils, a higher concentration of fibrils, or most likely a combination of

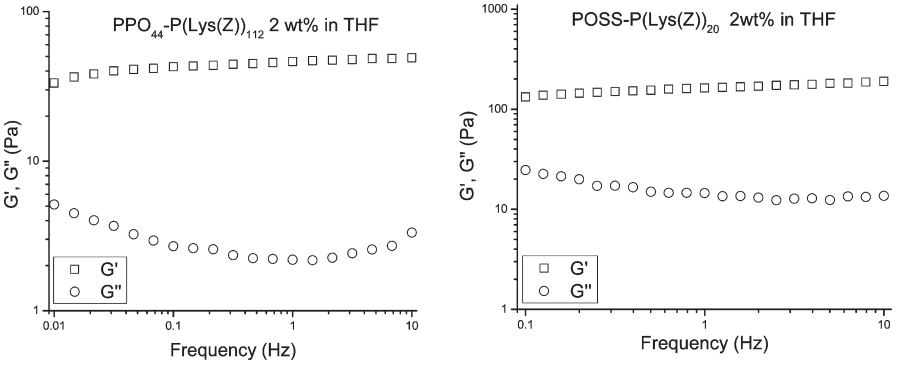

Figure 8. Representative frequency sweeps for PPO_{44}-$P(Lys(Z))_{112}$ (left) and POSS-$P(Lys(Z))_{20}$ (right) block copolymer organogels (2 wt % in THF). The data were taken under a controlled stress of 0.1 Pa at 2 °C. A frequency of 1 Hz (from previous experiments) is in the plateau region of G' from the frequency sweep.

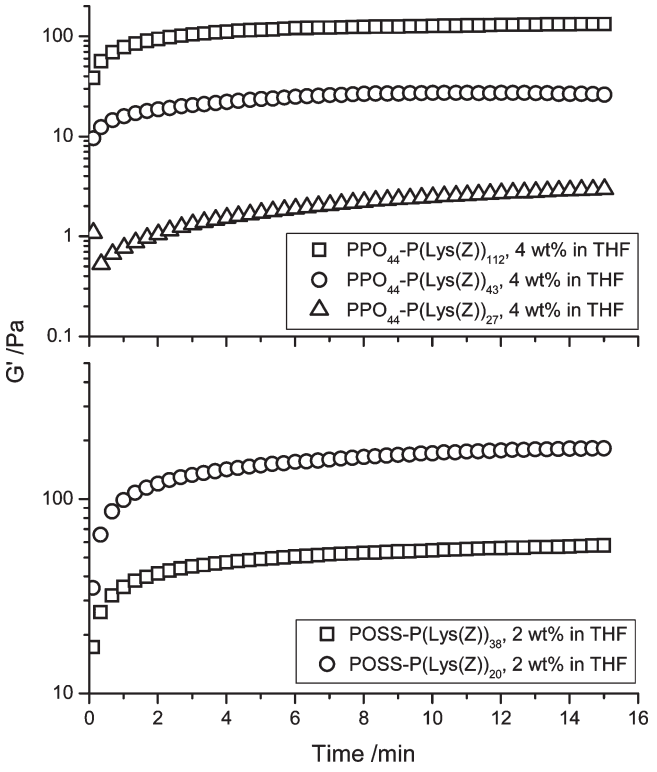

Figure 9. Recovery of P(Lys(Z)) organogels in THF after rigorous preshear (6 Hz, 2 min). (top) Recovery of 4 wt % solutions of PPO_{44}-$P(Lys(Z))_n$. (bottom) Recovery of 2 wt % solutions of POSS-$P(Lys(Z))_n$. Data were taken at 1 Hz under 0.1 Pa stress at 2 °C.

both. An increase in the modulus is indeed what is observed for PPO_{44}-$P(Lys(Z))_{112}$ as shown in Figure 6.

If we now consider the range in the linear viscoelastic response (i.e., the plateau region in the stress sweeps,) it appears that in general the critical stress required for the gels to begin thinning increases with increasing concentration and molecular weight. For example, in PPO- and POSS-based systems, the critical stress increases from ca. 2 to 40 Pa and ca. 60 to 70 Pa over the molecular weight range studied (Figure 5). For PPO_{44}-$P(Lys(Z))_{112}$ block copolymers the viscoelastic range increases from ca. 10 to 60 Pa over the concentration range from 1 to 4 wt % (Figure 6). If we again consider the assembly mechanism of intermolecular β-sheet formation, then these results make qualitative sense. In order to break assembled P(Lys(Z)) fibrils, the intermolecular contacts between peptide blocks would have to be broken. As the molecular weight or concentration increases, the magnitude and number of contacts per chain increase, resulting in a gel that can withstand thinning over a higher stress range. This explanation breaks down for PEOPO-P(Lys(Z)) block copolymers, where the viscoelastic range does not appear to increase with molecular weight even though the gel strength within the plateau region is higher. These systems in general formed much weaker gels, which may have an impact on their behavior. Coincidentally, the critical strain required for thinning appears to superpose for varying molecular weights of PPO-P(Lys(Z)) and POSS-P(Lys(Z)) (Figure 7). Above this critical strain the modulus decreases as the inverse square of the strain.

Recovery of Organogels. As mentioned above, P(Lys(Z))-based organogels in THF qualitatively appear to undergo a gel−sol transition at 77 °C based on a simple inversion of the test tube. The organogels appear to recover fully at low temperature. Rheologically, the P(Lys(Z)) organogels studied are shear thinning with frequency (Figure 8), as expected for physical gels.[45] We seek to determine the time scale for recovery of organogels after a rigorous preshear. Figure 9 shows the time sweeps for PPO-P(Lys(Z)) and POSS-P(Lys(Z)) organogels in 4 and 2 wt % THF, respectively, for various molecular weights. The time sweep shows that after complete breakdown the organogels nearly recover to the original gel strength over a 15 min time scale. Prior to prehear, PPO_{44}-$P(Lys(Z))_n$ organogels had strengths ca. 2.5, 43, and 220 Pa (for $n = 27$, 43, and 112, respectively). After recovery, the gel strengths were 3.8, 31, and 145 Pa. For POSS-$P(Lys(Z))_n$, the organogels had strengths ca. 70 and 170 Pa (for $n = 20$ and 38, respectively). After recovery, the gel strengths were 60 and 183 Pa. When considering PPO_{44}-$P(Lys(Z))_{112}$ organogels in THF as a function of concentration, the modulus changed from 8.7, 38, 57, and 220 Pa to 9, 36, 58, and 145 Pa after 15 min recovery for 1, 2, 3, and 4 wt % solutions, respectively. In general, the PPO-P(Lys(Z)) and POSS-P(Lys(Z)) organogels we able to recover fully. It is not clear why the 4 wt % PPO_{44}-$P(Lys(Z))_{112}$ system did not recover fully; however, there were systems where the strength post recovery was higher than the prepared samples. In particular, the 4 wt % PPO_{44}-$P(Lys(Z))_{27}$ organogel had not reached a constant strength after 15 min even though its recovered strength had already surpassed the original strength.

Effect of Adjacent Block on the Gel Strength. The results presented above focus on the relationship between organogel strength and the properties of the P(Lys(Z)) chain that facilitate strong intermolecular assembly via β-sheet interactions. There is also a clear dependence of organogel strength on the nonpeptide component in the copolymer. For example,

from the above results we see that the strength of the gels increases in going from PEOPO to PPO to POSS. In fact, the gel strength for 2 wt % POSS-P(Lys(Z)) in THF was higher compared with 4 wt % PPO-P(Lys(Z)) in THF. We propose a mechanism whereby the steric frustration introduced at the interface of the fibril assembly from the nonpeptide block serves to destabilize β-sheet assembly of the peptide block, resulting in a weaker gel. In the antiparallel β-sheet orientation, the N−H groups in the backbone of one strand hydrogen bond with the C═O groups in the backbone of the adjacent strands causing strong interchain interactions. Intramolecular hydrogen bonding within single β-strand is not possible.[46] On the other hand, formation of an antiparallel β-sheet is more likely for a polymer−peptide conjugate because this assembly motif allows the minimization of the steric repulsion of neighboring polymer coils.[37] Furthermore, it has been shown that the restriction of the conformational freedom in oligopeptide strands enhances the formation of antiparallel β-sheets.[47] In case of POSS-P(Lys(Z)), the P(Lys(Z)) chain has less freedom leading to formation of stronger gels. From the results above, 2 wt % solutions of POSS-P(Lys(Z)) formed the strongest gels in THF in terms of both gel strength and the range in the linear viscoelastic response. These copolymers also had the lowest critical gel concentrations. It is true that POSS molecules are highly soluble in THF and chloroform, and they are small enough that the interfacial area is minimized in the assembled structure. This facilitates close packing of the P(Lys(Z)) chains within the assembly, with the POSS cages in the corona serving to solubilize the fibrils. In fact, the gel strength of POSS-P(Lys(Z))$_{38}$ copolymers in chloroform was considerably stronger than in THF (348 vs 170 Pa for 2 wt % solutions.) Therefore, the solvent−POSS interactions are important in stabilizing the organogels (chloroform being a "better" solvent for POSS than THF.) When the non-peptide component is changed to PPO$_{44}$, the random configuration of the PPO chains at the interface of the assembly creates steric crowding, which disrupts the ability for P(Lys(Z)) blocks within the assembly to form strong intermolecular contacts; i.e., the P(Lys(Z)) block has more conformational freedom due to steric repulsion of neighboring chains. This results in a decreased gel strength as observed. When the PPO$_{44}$ is replaced with PEOPO$_{6-29}$ or PEOPO$_{10-31}$ (comparable degree of polymerization), the higher EO content makes THF a poorer solvent for that corona block.[48] The decrease in gel strength suggests that polymer−solvent interactions also play a key role on the strength of peptide organogels. Disruption of organogel structure due to changes at interface may also be caused chemically (i.e., through coupling or "click" reactions).[44,47] As an example, we have synthesized PPO-P(Lys(Z)) block copolymers through the copper-mediated alkyne−azide "click" chemistry between azido-PPO and alkyne-functionalized P(Lys(Z)). This block copolymer did not yield an organogel, potentially from the triazole ring at the interface.

Conclusions

We have studied organogelation in a series of P(Lys(Z))-based block copolymers with PPO, PEOPO, and POSS. Infrared spectroscopy indicates that the peptide block adopts an antiparallel β-sheet conformation whereby the assembly is facilitated by intermolecular H-bonding. It was found that increasing the P(Lys(Z)) molecular weight or concentration increases gel strength and the range of linear viscoelastic response with stress. Gel strengths as high as 220 and 348 Pa were observed in THF and chloroform, respectively. It is remarkable that such low concentrations of gelators (in this case ca. 2 wt % POSS-P(Lys(Z))) were able to form such strong gels in very low surface tension solvents. Finally, we observed that the gel strength is highly dependent on the solvent interactions with the non-peptide block of the copolymer. We attribute this to the conformational freedom in the P(Lys(Z)) chain, which serves to destabilize β-sheet assembly of peptide block, leading to weaker gel.

Acknowledgment. The authors gratefully acknowledge start-up funding from USM. We thank Dr. Sateesh Peddini, Amol Nalawade, and Prof. Kenneth Mauritz for use of their FTIR and for useful discussion as well as Stephen Foster and Prof. Robert Lochhead for use of their rheometer and for useful discussions.

Supporting Information Available: NMR spectra for the Lys(Z)−NCA and a description of the PPO−OH conversion to PPO−NH_2. This material is available free of charge via the Internet at http://pubs.acs.org.

References and Notes

(1) Treanor, R. L.; Weiss, R. G. *J. Am. Chem. Soc.* **1986**, *108* (11), 3137–9.
(2) Lin, Y. C.; Kachar, B.; Weiss, R. G. *J. Am. Chem. Soc.* **1989**, *111* (15), 5542–51.
(3) Pochan, D. J.; Schneider, J. P.; Kretsinger, J.; Ozbas, B.; Rajagopal, K.; Haines, L. *J. Am. Chem. Soc.* **2003**, *125* (39), 11802–11803.
(4) Schneider, J. P.; Pochan, D. J.; Ozbas, B.; Rajagopal, K.; Pakstis, L.; Kretsinger, J. *J. Am. Chem. Soc.* **2002**, *124* (50), 15030–15037.
(5) Gebhardt, K. E.; Ahn, S.; Venkatachalam, G.; Savin, D. A. *Langmuir* **2007**, *23* (5), 2851–2856.
(6) Gebhardt, K. E.; Ahn, S.; Venkatachalam, G.; Savin, D. A. *J. Colloid Interface Sci.* **2008**, *317* (1), 70–76.
(7) Horkay, F.; Tasaki, I.; Basser, P. J. *Biomacromolecules* **2001**, *2* (1), 195–9.
(8) Nam, K.; Watanabe, J.; Ishihara, K. *Int. J. Pharm.* **2004**, *275* (1−2), 259–269.
(9) Qu, X.; Wirsen, A.; Albertsson, A.-C. *J. Appl. Polym. Sci.* **1999**, *74* (13), 3186–3192.
(10) Petka, W. A.; Hardin, J. L.; McGrath, K. P.; Wirtz, D.; Tirrell, D. A. *Science* (*Washington, DC, U. S.*) **1998**, *281* (5375), 389–392.
(11) Deming, T. J. *Soft Matter* **2005**, *1* (1), 28–35.
(12) Deming, T. J. *Prog. Polym. Sci.* **2007**, *32* (8−9), 858–875.
(13) Breedveld, V.; Nowak, A. P.; Sato, J.; Deming, T. J.; Pine, D. J. *Macromolecules* **2004**, *37* (10), 3943–3953.
(14) Kim, K. T.; Park, C.; Vandermeulen, G. W. M.; Rider, D. A.; Kim, C.; Winnik, M. A.; Manners, I. *Angew. Chem., Int. Ed.* **2005**, *44* (48), 7964–7968.
(15) Diaz, N.; Simon, F.-X.; Schmutz, M.; Rawiso, M.; Decher, G.; Jestin, J.; Mesini, P. J. *Angew. Chem., Int. Ed.* **2005**, *44* (21), 3260–3264.
(16) Gao, P.; Zhan, C.; Liu, L.; Zhou, Y.; Liu, M. *Chem. Commun.* (*Cambridge, U. K.*) **2004**, *10*, 1174–1175.
(17) George, M.; Snyder Samuel, L.; Terech, P.; Glinka Charles, J.; Weiss Richard, G. *J. Am. Chem. Soc.* **2003**, *125* (34), 10275–83.
(18) Ryu, S. Y.; Kim, S.; Seo, J.; Kim, Y.-W.; Kwon, O.-H.; Jang, D.-J.; Park, S. Y. *Chem. Commun.* (*Cambridge, U. K.*) **2004**, *21*, 70–71.
(19) Shumburo, A.; Biewer, M. C. *Chem. Mater.* **2002**, *14* (9), 3745–3750.
(20) Sone, E. D.; Zubarev, E. R.; Stupp, S. I. *Angew. Chem., Int. Ed.* **2002**, *41* (10), 1705–1709.
(21) Tew, G. N.; Pralle, M. U.; Stupp, S. I. *J. Am. Chem. Soc.* **1999**, *121* (42), 9852–9866.
(22) Zhan, C.; Gao, P.; Liu, M. *Chem. Commun.* (*Cambridge, U. K.*) **2005**, *4*, 462–464.
(23) Zhan, C.; Wang, J.; Yuan, J.; Gong, H.; Liu, Y.; Liu, M. *Langmuir* **2003**, *19* (22), 9440–9445.
(24) Markland, P.; Zhang, Y.; Amidon, G. L.; Yang, V. C. *J. Biomed. Mater. Res.* **1999**, *47* (4), 595–602.
(25) Suzuki, M.; Nakajima, Y.; Yumoto, M.; Kimura, M.; Shirai, H.; Hanabusa, K. *Org. Biomol. Chem.* **2004**, *2* (8), 1155–1159.
(26) Suzuki, M.; Sato, T.; Kurose, A.; Shirai, H.; Hanabusa, K. *Tetrahedron Lett.* **2005**, *46* (16), 2741–2745.
(27) Terech, P.; Weiss, R. G. *Chem. Rev.* (*Washington, DC, U. S.*) **1997**, *97* (8), 3133–3159.

(28) Van Esch, J. H.; Feringa, B. L. *Angew. Chem., Int. Ed.* **2000**, *39* (13), 2263–2266.
(29) Escuder, B.; Miravet, J. F. *Langmuir* **2006**, *22* (18), 7793–7797.
(30) Zubarev, E. R.; Pralle, M. U.; Sone, E. D.; Stupp, S. I. *J. Am. Chem. Soc.* **2001**, *123* (17), 4105–4106.
(31) Kim, K. T.; Vandermeulen, G. W. M.; Winnik, M. A.; Manners, I. *Macromolecules* **2005**, *38* (12), 4958–4961.
(32) Kuo, S.-W.; Lee, H.-F.; Huang, C.-F.; Huang, C.-J.; Chang, F.-C. *J. Polym. Sci., Part A: Polym. Chem.* **2008**, *46* (9), 3108–3119.
(33) Kuo, S.-W.; Lee, H.-F.; Huang, W.-J.; Jeong, K.-U.; Chang, F.-C. *Macromolecules* **2009**, *42* (5), 1619–1626.
(34) Papadopoulos, P.; Floudas, G.; Klok, H. A.; Schnell, I.; Pakula, T. *Biomacromolecules* **2004**, *5* (1), 81–91.
(35) Cho, C. S.; Jeong, Y. I.; Kim, S. H.; Nah, J. W.; Kubota, M.; Komoto, T. *Polymer* **2000**, *41* (14), 5185–5193.
(36) Kim, K. T.; Park, C.; Kim, C.; Winnik, M. A.; Manners, I. *Chem. Commun.* (*Cambridge, U. K.*) **2006**, *13*, 1372–1374.
(37) Hentschel, J.; Boerner, H. G. *J. Am. Chem. Soc.* **2006**, *128* (43), 14142–14149.
(38) Hirst, A. R.; Smith, D. K.; Feiters, M. C.; Geurts, H. P. M. *Langmuir* **2004**, *20* (17), 7070–7077.
(39) Partridge, K. S.; Smith, D. K.; Dykes, G. M.; McGrail, P. T. *Chem. Commun.* (*Cambridge, U. K.*) **2001**, No. 4, 319–320.
(40) Estroff, L. A.; Hamilton, A. D. *Chem. Rev.* (*Washington, DC, U. S.*) **2004**, *104* (3), 1201–1217.
(41) Van Dijk-Wolthuis, W. N. E.; Van de Water, L.; Van de Wetering, P.; Van Steenbergen, M.; Kettenes-Van den Bosch, J. J.; Schuyl, W.; Hennink, W. E. *Macromol. Chem. Phys.* **1997**, *198* (12), 3893–3906.
(42) Diaz, D. D.; Finn, M. G. *Chem. Commun. (Cambridge, U. K.)* **2004**, *21*, 2514–2516.
(43) Mauerer, A.; Lee, G. *Eur. J. Pharm. Biopharm.* **2006**, *62* (2), 131–142.
(44) Tzokova, N.; Fernyhough, C. M.; Butler, M. F.; Armes, S. P.; Ryan, A. J.; Topham, P. D.; Adams, D. J. *Langmuir* **2009**, ASAP (DOI: 10.1021/la901413n).
(45) Terech, P.; Pasquier, D.; Bordas, V.; Rossat, C. *Langmuir* **2000**, *16* (10), 4485–4494.
(46) Oku, H.; Yamada, K.; Katakai, R. *Biopolymers* **2008**, *89* (4), 270–283.
(47) Eckhardt, D.; Groenewolt, M.; Krause, E.; Borner Hans, G. *Chem. Commun.* (*Cambridge, U. K.*) **2005**, No. 22, 2814–6.
(48) Brandrup, J.; Immergut, E. H.; Grulke, E. A. *Polymer Handbook*, 4th ed.; John Wiley and Sons: Hoboken, NJ, 1999; Vol. *1*.
(49) Chen, Q.; Zhang, D.; Zhang, G.; Zhu, D. *Langmuir* **2009**, ASAP (DOI: 10.1021/la9016257).